Title

Identification of Novel Glucocerebrosidase Chaperones by Unexpected Skeletal Rearrangement Reaction

Authors

Kunitoshi Takeda[a], Toru Watanabe[a], James Smith[b], David Vesey[b], Nathalie Tiberghien[b], Sian Lewis[a], Ben Powney[a], Anthony H. V. Schapira[c], Tamaki Hoshikawa*[a], Andrew K. Takle[a]

[a] Hatfield Research Laboratories, Eisai Ltd., Hatfield, AL10 9SN, United Kingdom

[b] Charles River Laboratories, 7-9 Spire Green Centre, Flex Meadow, Harlow, Essex, CM19 5TR, United Kingdom

[c] Department of Clinical and Movement Neurosciences, UCL Queen Square Institute of Neurology, University College London, London, United Kingdom

[*] To whom correspondence should be addressed: Tamaki Hoshikawa, Hatfield Research Laboratories, Eisai Ltd., Hatfield, AL10 9SN, United Kingdom, t-hoshikawa@hhc.eisai.co.jp

Keywords

Glucocerebrosidase

Pharmacological chaperone

Parkinson disease

Gaucher Disease

Abstract

Glucocerebrosidase (GCase), encoded by GBA1 gene, is a lysosomal enzyme catalysing the hydrolysis of glucosylceramide into glucose and ceramide. Genetic variants of GBA1 that lead to dysfunctional GCase, cause a lysosomal storage disorder known as Gaucher disease (GD). Heterozygous variants of GBA1 are also known as the most common genetic risk factor associated with Parkinson's disease (PD). Compound **5** was identified as a primary hit from a high-throughput screening campaign to identify small molecule pharmacological chaperones as positive modulators of GCase function. Further studies revealed that compound **5** was slowly transformed into compound **6** in PBS buffer *via* an unexpected skeletal rearrangement. Optimisation of compound **6** yielded a series of potent GCase pharmacological chaperones as exemplified by compound **38**.

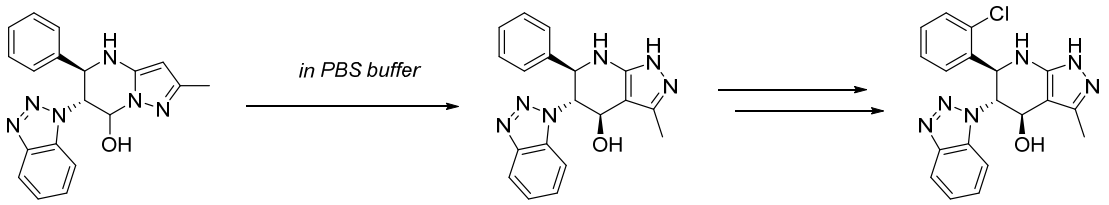

5 (HTS hit)
unstable in PBS buffer

***rac*-6**
stable
EC_{50} = 1.4 μM

***rac*-38**
EC_{50} = 0.14 μM

Gaucher disease (GD) is the most common lysosomal storage disease caused by mutations of the GBA1 gene, which encodes the lysosomal enzyme glucocerebrosidase (GCase), responsible for the conversion of glucosylceramide into glucose and ceramide. It is postulated that disease associated GCase variants are misfolded leading to a reduction of functional GCase protein in the lysosome. Deficiencies in GCase function, which leads to abnormal accumulation of its substrate glucosylceramide, is the underlying feature of GD.[1] GD is categorized into three different types based on the clinical symptoms, age at onset, and rate of progression.[2] Type 1 GD is the most common and characterised by splenomegaly, blood disorders such as anaemia and low levels of blood platelets, osteoporosis and the lack of neurological symptoms. Type 2 and type 3 GD are characterised by neurological impairments, where type 3 GD usually starts at later age with slower progression than type 2 GD. Enzyme replacement therapy and substrate reduction therapy are accepted treatment strategies for some patients with type 1 GD, but there are still unmet needs particularly those associated with GCase dysfunction within the central nervous system. In addition, mutations of the GBA1 gene are the most common genetic risk factor for Parkinson's disease (PD) and Dementia with Lewy Bodies (DLB), supporting additional needs for development of brain penetrant therapeutic agents.[3]

Pharmacological chaperones (PCs) are small molecules which facilitate the correct folding of proteins. Brain penetrant small molecule GCase PCs are expected to facilitate GCase refolding and subsequent trafficking to the lysosome, and have been proposed as an alternative therapeutic strategy.[4] PCs have the potential to not only increase lysosomal GCase but also to decrease accumulation of misfolded GCase which has been postulated to cause endoplasmic reticulum (ER) stress, mitochondrial disfunction, increased inflammatory responses, and decreased chaperone mediated autophagy.[5, 6] Several GCase PCs have previously been reported, including iminosugar compounds exemplified by isofagomine (IFG, **1**)[7] and non-iminosugars exemplified by compound **2**[8], **3**[9], and **4**[10] (Fig. 1).

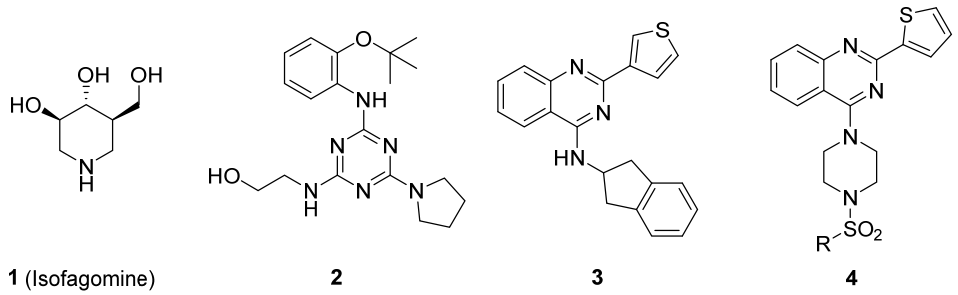

1 (Isofagomine) **2** **3** **4**

Figure 1. Structure of representative GCase pharmacological chaperones

We sought to identify novel GCase PCs by performing a high-throughput screen (HTS) in a GBA N370S/null patient-derived fibroblast cell line using GCase activity following cell lysis as a surrogate measure of GCase protein levels,[11] and identified compound **5** (Fig. 2) as a hit with moderate chaperoning activity (EC_{50} 5.6 μM) following 5-days of compound treatment. Compound **5**, which proved to be a diastereomeric mixture at the hydroxyl group as determined by NMR spectroscopy,[12] had an intriguing structure but one which raised concerns due to the potential instability of the hemiaminal moiety. We discovered that compound **5** was stable in either acidic buffer[13] or DMSO, but that it slowly transformed into the regio-isomeric compound **6**, in a stereo-selective manner, after 5-day storage at 37 °C in pH 7.4 aqueous phosphate buffer. As these latter conditions mimic those of the HTS, it was proposed that compound **5** could be transformed into **6** during the 5-day assay.

The proposed mechanism of the transformation of **5** to **6** was ring-opening of the hemiaminal, bond rotation, followed by an intramolecular Friedel-Crafts like carbon-carbon bond formation between the

amino pyrazole and aldehyde as shown in Fig. 2.[14,15] The equilibrium between hemiaminal and aldehyde was also supported by the fact that compound **5** underwent a reduction by $NaBH_4$ to provide a ring-opened alcohol **7**. Furthermore, an authentic sample of compound **6** retained chaperoning activity (EC_{50} 1.4 μM), whereas compound **8**, which was unable to undergo the proposed rearrangement, was devoid of activity in the GCase chaperoning assay. Although the true chaperoning activity of HTS hit **5** itself was still inconclusive, we decided to start further optimisation from compound **6** due to its proven activity and chemical stability.

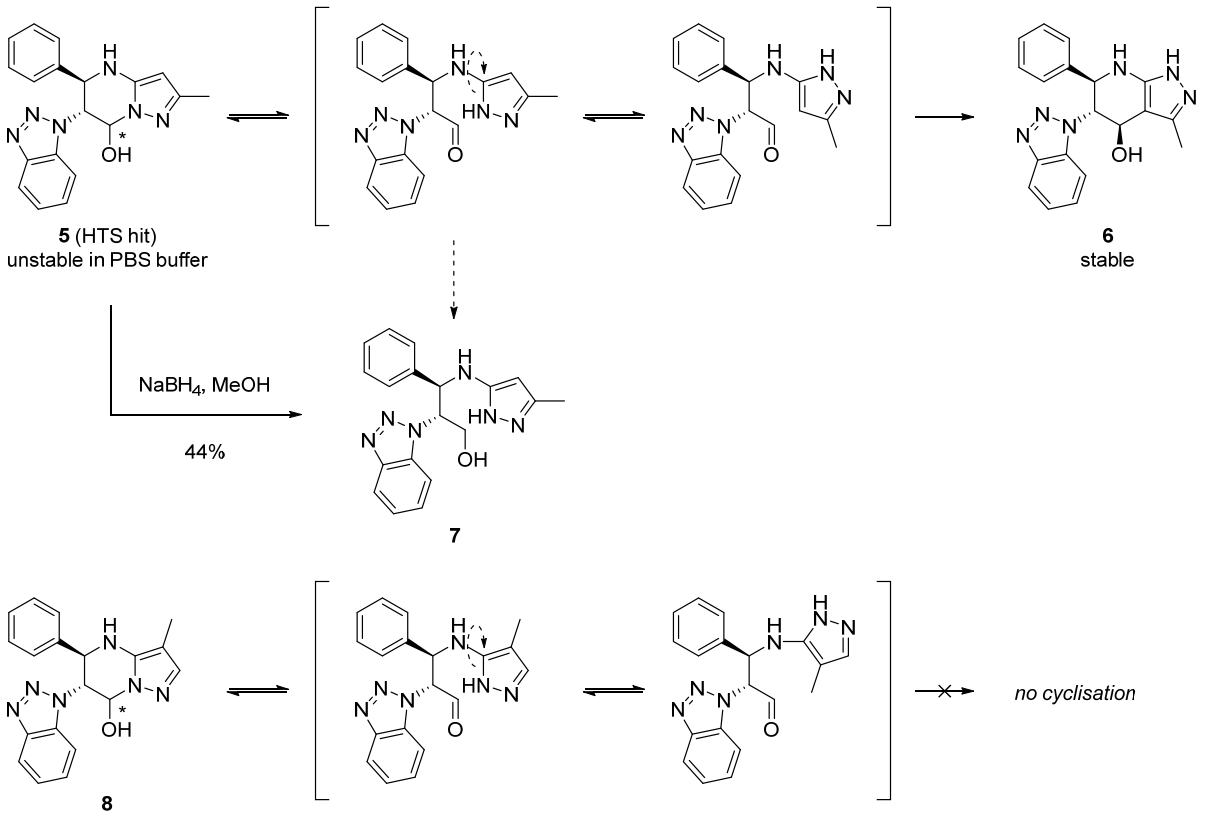

Figure 2. Proposed mechanism for the transformation of compound **5** to **6**

In seeking to explore the structure-activity relationships (SAR) of compound **6,** we synthesised analogues using the general synthetic route shown in Scheme 1, which exploits the rearrangement described above.[16] The intermediate acyclic aldehydes **11** were prepared from acetal **9** using a method analogous to that reported by Katritzky et al.[17] Compound **11** was reacted with 3-substituted 5-aminopyrazoles to afford intermediate **12** as an inseparable diastereomeric mixture. Rearrangement to compound **13** was conducted using the mildly acidic solvent, 1,1,1,3,3,3-hexafluoro-2-propanol, which was reported as mild and efficient conditions for Friedel-Crafts reaction by Aubé et al.[18] In this reaction, compound **13** was obtained as a single diastereomer, suggesting this rearrangement reaction proceeded in a stereo-selective manner to avoid steric repulsion between R^1 and the benzotriazole substituent. Chiral separation could be achieved using HPLC and Daicel CHIRALPAK® IE to afford the enantiomers **14** and **15**.

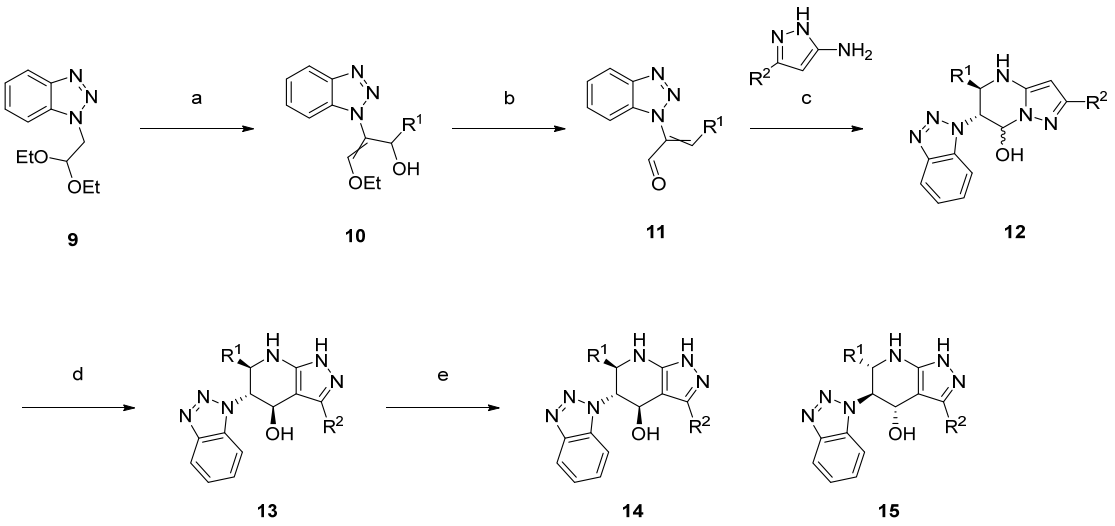

Scheme 1. General method for the synthesis of analogues of compound **6**. Reagents and conditions: a) R^1CHO, *n*-BuLi, THF, -78 °C; b) 2M aqueous HCl, THF, 50 - 60 °C; c) EtOH, EtOH-DCM, or 2-BuOH, rt to 50 °C; d) 1,1,1,3,3,3-hexafluoro-2-propanol, rt to 50 °C; e) chromatographic separation by chiral HPLC

Alternative synthetic routes were required for the synthesis of analogues where the pyrazole unit was replaced by other aromatic rings. The synthesis of the benzo-fused compound **20** is described in Scheme 2. An S_N2 substitution reaction of the commercially available bromoketone **16** with benzotriazole was conducted in the presence of NaOH to obtain **17** in 73% yield. Condensation with benzaldehyde gave the enone **18** in 46% yield. The nitro group was then reduced with iron powder which also caused an intramolecular cyclisation to produce ketone **19** in 67% yield as a single diastereomer, which suggested that the cyclization proceeded in a stereo-selective manner. Reduction of **19** with DIBAL afforded the desired compound **20** in 62% yield as a 92:8 diastereomixture (major isomer as drawn).

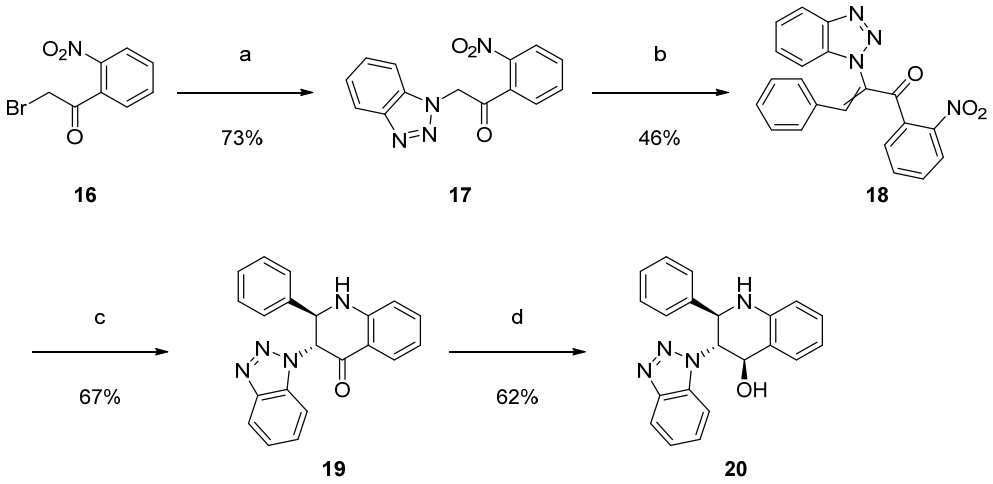

Scheme 2. Synthesis of compound **20**. Reagents and conditions: a) Benzotriazole, NaOH, DMF, reflux; b) PhCHO, piperidine, EtOH, rt; c) Fe, AcOH, EtOH, 60 °C; d) DIBAL, THF, rt.

The 7-aza analogue **25** was synthesised using a slight modification of the route above (Scheme 3). Compound **22** was prepared in 62% yield by treating acid chloride **21** with trimethylsilyl methyl benzotriazole using a method analogous to that reported by Katritzky et al.[19] The subsequent three steps

(b, c, and d) were conducted using similar reaction conditions described in Scheme 2 to obtain compound **25**.

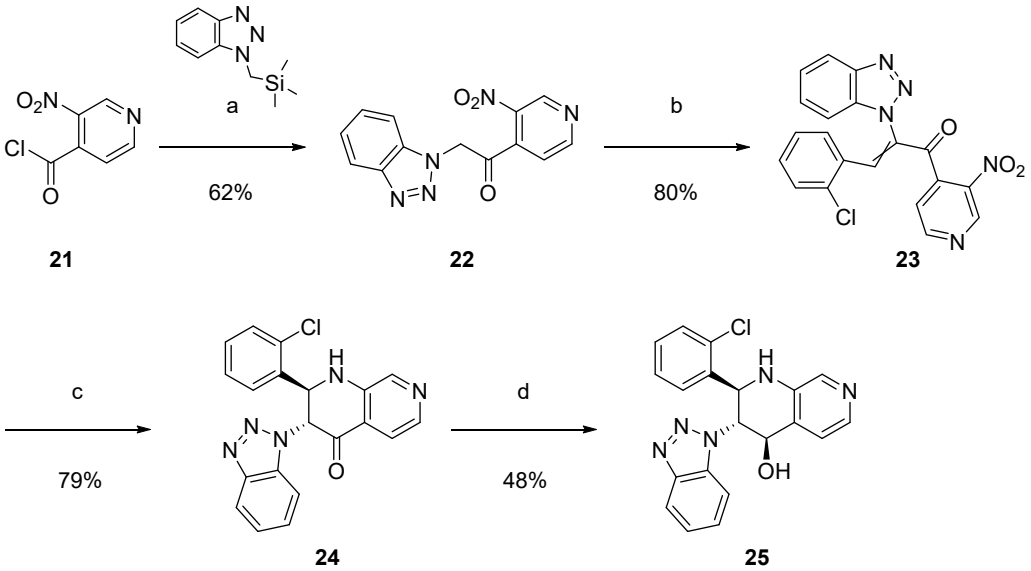

Scheme 3. Synthesis of compound **25**. Reagents and conditions: a) THF, reflux; b) 2-Chlorobenzaldehyde, piperidine, EtOH, 75 °C; c) Fe, AcOH, EtOH, 60 °C; d) DIBAL, THF, rt.

The isomeric 6-aza derivative **31** was synthesised by the route described in Scheme 4. Treatment of aldehyde **26** with trimethylsilyl methyl benzotriazole afforded the alcohol **27**. Oxidation of the alcohol using Dess-Martin periodinane followed by condensation with 2-chlorobenzaldehyde gave compound **29** in 28% yield over 3 steps. Removal of the Boc protecting group in TFA gave a crude unprotected amine intermediate, which was heated at 50 °C in the presence of Et_3N to provide the cyclic ketone **30** in 66% yield as a 83:17 mixture of *trans*/*cis* diastereomers. Reduction of the ketone with DIBAL afforded compound **31** in 34% yield as a 86:14 diastereomixture (major isomer as drawn).

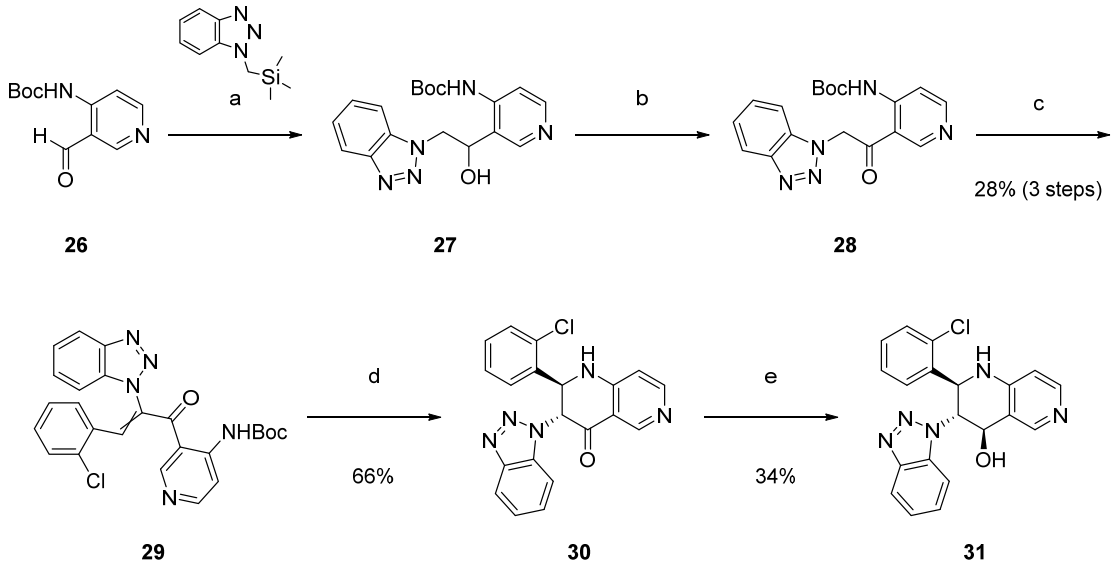

Scheme 4. Synthesis of compound **31**. Reagents and conditions: a) TBAF, THF, rt; b) Dess-Martin periodinane, DCM, rt; c) 2-Chlorobenzaldehyde, piperidine, EtOH, rt; d) TFA, DCM, rt, then Et_3N, 2-BuOH, 50 °C; e) DIBAL, THF, rt.

The chaperoning activity of the novel compounds was evaluated by measurement of GCase activity using the fluorescent substrate 4 methylumbelliferyl-β-D-glucopyranoside (4-MUG),[20] following 5-day compound treatment of a GBA N370S/null patient-derived fibroblast cell line. The chaperoning potency (EC_{50}) and efficacy (Emax), normalised to the positive control IFG (100%) and DMSO control (0%), were used to assess the activity of each compound.

Our SAR investigations began by exploring the effect of substitution on the phenyl ring (Table 1). The introduction of methyl or fluoro substituents at 2-, 3-, or 4-position had little impact on potency or efficacy (compounds **32**-**37**). Introduction of a 2-chloro substituent (**38**) however, increased potency by approximately 10-fold compared to compound **6**. The 2-bromo (**39**) and 2-trifluoromethyl (**40**) analogues also showed improved activity whereas the 2-methoxy analogue (**41**) was less active. 2,3-disubstitution (compounds **42**-**44**) also showed improved activity, comparable to compound **38**. However, the 2,4- and 2,5-dichloro analogues (**45** and **46**) showed no significant improvements in activity compared to compound **6**.

Table 1. SAR investigation of the phenyl substituent

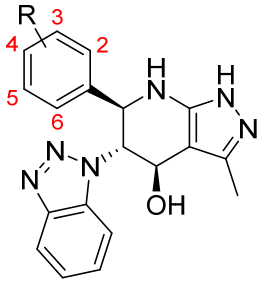

		Chaperone activity	
Compound	R	EC_{50} (μM)	Emax (%)
6	H	1.4	173
32	2-Me	1.9	158
33	3-Me	1.1	158
34	4-Me	1.1	157
35	2-F	0.97	137
36	3-F	1.2	137
37	4-F	2.2	61
38	2-Cl	0.14	160
39	2-Br	0.20	164
40	2-CF_3	0.47	160
41	2-OMe	3.3	>140
42	2-Cl, 3-Me	0.15	147
43	2-Cl, 3-F	0.11	148

44	2,3-diCl	0.14	140
45	2,4-diCl	0.74	150
46	2,5-diCl	0.72	145

All the compounds in this table are racemic.

The impact of chirality on chaperoning activity was explored following chiral separation of compounds **6**, **38**, and **39** (Table 2). In each case, all activity resided in a single enantiomer and the other was devoid of activity (**47** vs **48**, **49** vs **50**, and **51** vs **52**). The absolute *S,S,S* configuration of compound **48** was determined by X-ray crystallography (Fig. 3), from which we inferred that all activity resided in the *R*, *R*, *R* enantiomer.

Table 2. Activity comparison between enantiomers

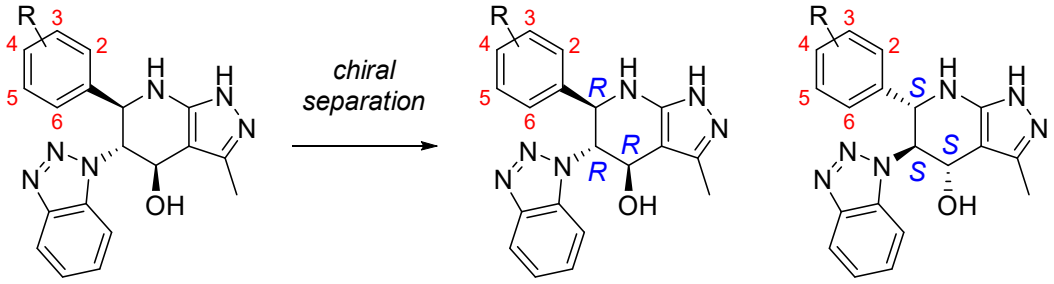

		Chaperone activity	
Compound	R	EC_{50} (μM)	Emax (%)
6	H	1.4	173
47 (*R*, *R*, *R*)	H	1.1	137
48 (*S*, *S*, *S*)	H	inactive	N/S
38	2-Cl	0.14	160
49 (chiral)	2-Cl	0.076	163
50 (chiral)	2-Cl	inactive	N/S
39	2-Br	0.20	164
51 (chiral)	2-Br	0.086	170
52 (chiral)	2-Br	inactive	N/S

Compounds **6**, **38**, and **39** in this table are racemic. N/S means no significant effect.

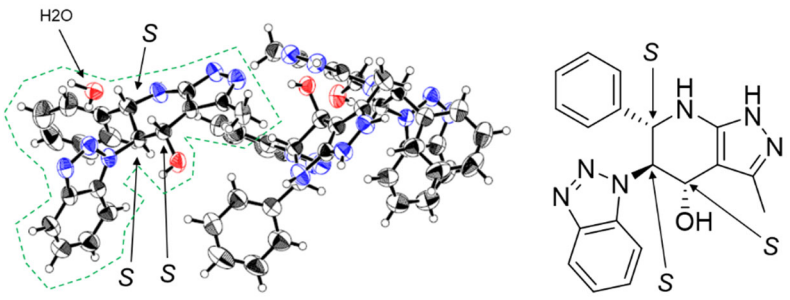

Figure 3. Determination of absolute configuration of compound **48**

Replacement of the phenyl substituent on the piperidine core was also explored (Table 3). Replacement with small alkyl substituents (compounds **53** and **54**) led to a loss of activity but the larger cyclo-pentyl derivative (**55**) showed similar activity to compound **6**. The cyclohexyl- (**56**) and cycloheptyl- (**57**) derivatives exhibited more potent activity, whereas the 4-tetrahydropyranyl (4-THP) derivative **58** resulted in significantly reduced activity. These results suggested an aromatic substituent was not essential and could be replaced by a similarly sized (or larger) hydrophobic group.

Table 3. Replacement of the phenyl substituent

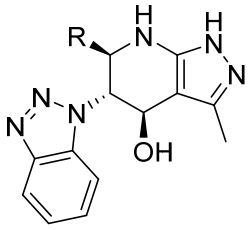

		Chaperone activity	
Compound	R	EC_{50} (μM)	Emax (%)
6	Ph	1.4	173
53	Me	inactive	N/S
54	cyc-Propyl	inactive	N/S
55	cyc-Pentyl	1.9	150
56	cyc-Hexyl	0.37	180
57	cyc-Heptyl	0.23	170
58	4-THP	14	>80

All the compounds in this table are racemic. N/S means no significant effect.

We next explored the effect of substitution on the pyrazole ring (Table 4). Removal of the methyl group significantly diminished the activity (**59** vs **6**). However, replacement with an ethyl substituent (**60**) retained activity albeit slightly reduced when compared to **38**, and the cyclo-propyl derivative (**61)** showed comparable activity to compound **38** . The larger tert-butyl (**62**) showed significantly reduced activity, whereas the cyclo-pentyl (**63**), phenyl (**64**) and methoxymethyl analogues (**65**) were inactive.

Table 4. Effects of pyrazole substitution

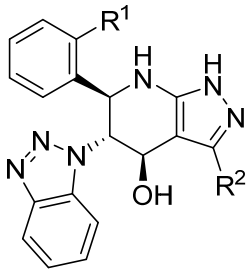

			Chaperone activity	
Compound	R^1	R^2	EC_{50} (μM)	Emax (%)
6	H	Me	1.4	173
38	Cl	Me	0.14	160
59	H	H	inactive	>40
60	Cl	Et	0.48	191
61	Cl	cyc-propyl	0.083	172
62	Cl	tert-Bu	7.4	132
63	H	cyc-Pentyl	inactive	N/S
64	Cl	phenyl	inactive	N/S
65	H	methoxymethyl	inactive	N/S

All the compounds in this table are racemic. N/S means no significant effect.

Next, the effect of replacement of the fused pyrazole moiety was explored (Table 5). Replacement with a phenyl group (**20**) or its 6-aza analogue (**31**) was not tolerated, whereas the 7-aza analogue (**25**) possessed potent chaperoning activity.

Table 5. Pyrazole replacements

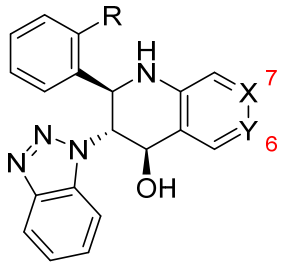

				Chaperone activity	
Compound	R	X	Y	EC_{50} (μM)	Emax (%)
20	H	C	C	inactive	N/S
25	Cl	N	C	0.57	151
31	Cl	C	N	7.4	>340

All the compounds in this table are racemic. N/S means no significant effect.

We have previously reported the importance of fully characterising potential GCase pharmacological chaperones using cell penetrant probes.[11] GCase pharmacological chaperones that bind at or in the vicinity of the GCase active site can paradoxically also act as enzyme inhibitors. The 4-MUG GCase activity assay may underrepresent this GCase inhibitory activity as test compounds can potentially be diluted or washed out during the cell lysis protocol. We therefore investigated the activity of a selection of our most potent GCase chaperones in a whole-cell assay using the cell penetrant fluorescent GCase substrate 5-(pentafluorobenzoylamino)fluorescein di-β-D-glucopyranoside (PFB-FDGlu).[21] Data are compared to IFG **1** (Table 6). All compounds with GCase chaperoning activity also showed in-cell GCase inhibition, with no significant separation between the chaperoning and inhibitory activity. Indeed,

as shown in Figure 4, there is a clear correlation between these activities. This was also supported by the fact that the *S*, *S*, *S*-isomer **48**, the inactive counterpart of *R*, *R*, *R*-isomer **47**, did not display any in-cell GCase inhibitory activity.

Table 6. Comparison of chaperoning and inhibitory activity

	Chaperone activity		In-cell inhibition	
Compound	EC_{50} (μM)	Emax (%)	IC_{50} (μM)	Emax (%)
1 (IFG)	0.30	103	0.41	103
47	1.1	137	3.2	95
32	1.91	158	4.6	>80
35	0.97	137	1.8	103
49	0.076	163	0.11	85
51	0.086	170	0.33	101
40	0.47	160	1.1	103
56	0.37	180	0.65	102
61	0.083	172	0.074	95
25	0.57	151	1.8	99
48	inactive	N/S	inactive	N/S

Both chaperone and inhibitory activities were determined in patient-derived fibroblasts bearing the N370S GBA mutation.

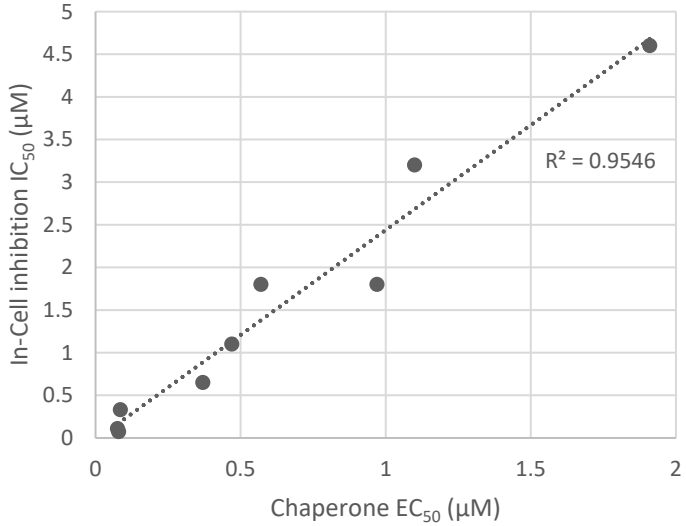

Figure 4. Correlation between chaperone EC_{50} and in-cell inhibition IC_{50} (compounds in Table 6 except for IFG and **48**)

Finally, in order to assess drug-likeness of this series, solubility, liver microsomal stability (LMS), and hERG (human Ether-à-go-go-Related Gene) inhibition were evaluated for representative compounds (Table 7). All the compounds showed >100 μM solubility in both neutral and acidic buffer solution. Also, no significant microsomal stability issues were found in either the human or mouse systems. Compounds **49** and **51** also showed no significant hERG inhibitory activities (IC_{50} >25μM).

Table 7. Solubility, Liver Microsomal Stability, and hERG inhibition

	Solubility (μM)		LMS Clint (μl/min/mg)		hERG IC_{50}
Compound	pH 7.4	pH 1.2	human	mouse	(μM)
47	>100	>100	5.01	9.88	NT
49	>100	>100	9.61	15.7	>25
51	>100	>100	22.7	31.4	>25

NT means not tested.

In summary, compound **6** was identified as a novel GCase chaperone by HTS screening and subsequent chemical investigation of the original hit compound **5**. We have presented a summary of our SAR investigations which resulted in the discovery of compound **38** which displayed greater GCase chaperoning potency than IFG in a 5-day cell-lysate GCase activity assay. Although compound characterization using an in-cell GCase activity assay revealed that this series of compounds were also GCase inhibitors, further studies could be carried out to understand the net benefits of GCase modulation within an *in vivo* setting. The results of solubility, LMS stability, and hERG inhibition assays supported that this series of compounds had good drug-like profiles.

Acknowledgement

The authors appreciate Masaki Kato for the determination of absolute stereochemistry of compound **48** by X-ray crystal structure analysis, and So Yasui for structural analysis of compound **5** as well as collecting high-resolution mass spectrometry data and ^{13}C NMR.

1 **References**

[1] Stirnemann J.; Belmatoug N.; Camou F.; Serratrice C.; Froissart R.; Caillaud C.; Levade T.; Astudillo L.; Serratrice J.; Brassier A.; Rose C.; Billette de Villemeur T.; Berger M. G. *Int. J. Mol. Sci.* **2017**, *18*, 441.
[2] Baris, H. N.; Cohen I. J.; Mistry P. K. *Pediatr Endocrinol Rev.* **2014**, *12 Suppl 1*, 72.
[3] Gegg M. E.; Menozzi E.; Schapira A. H. V. *Neurobiol. Dis.* **2022**, *166*, 105663.
[4] Butters T. D. *Curr. Opin. Chem. Biol.* **2007**, *11*, 412.
[5] Han T-U.; Sam R.; Sidransky E. *Front. Cell Dev. Biol.* **2020**, *8*, 271.
[6] Horowitz M.; Braunstein H.; Zimran A.; Revel-Vilk, S.; Goker-Alpan, O. *Adv Drug Deliv Rev.* **2022**, *187*, 114402.
[7] Steet R. A.; Chung S.; Wustman B.; Powe A.; Do H.; Kornfeld S. A. *Proc. Natl. Acad. Sci. USA* **2006**, *103*, 13813.
[8] Huang W.; Zheng W.; Urban D. J.; Inglese J.; Sidransky E.; Austin C. P.; Thomas C. J. *Bioorg. Med. Chem. Lett.* **2007**, *17*, 5783.
[9] Zheng J.; Chen L.; Schwake M.; Silverman R. B.; Krainc D. *J. Med. Chem.* **2016**, *59*, 8508.
[10] Marugan J. J.; Zheng W.; Motabar O.; Southall N.; Goldin E.; Westbroek W.; Stubblefield B.; Sidransky E.; Aungst R.; Lea W. A.; Simeonov A.; Leister W.; Austin C. P. *J. Med. Chem.* **2011**, *54*, 1033.
[11] Hoshikawa T.; Watanabe T.; Kotake M.; Tiberghien N.; Woo C.-K.; Lewis S.; Thomas B.; Koglin M.; Staddon J. M.; Powney B.; Schapira A. H. V.; Takle A. K. *Bioorg. Med. Chem. Lett.* **2023**, *81*, 129130.
[12] Compound **5** was originally purchased from a commercial supplier and the structure was confirmed by 2D NMR experiments.
[13] Stability was tested in JP1 fluid (Japanese Pharmacopoeia Dissolution Test Fluid No. 1, pH 1.2).
[14] Choi P. J.; Lu G-L.; Sutherland H. S.; Giddens A. C.; Franzblau S. G.; Cooper C. B.; Denny W. A.; Palmer B. D. *Tetrahedron Lett.* **2022**, *90*, 153611.
[15] Goryaeva M. V.; Burgart, Y. V.; Saloutin V. I. *J. Fluor. Chem.* **2013**, *147*, 15.
[16] Detailed experimental procedures are available in the Supplementary Information.
[17] Katrizky A. R.; Vakulenko A. V.; Akue-Gedu R.; Gromova A. V.; Witek R.; Rogers J. W. *Arkivoc* **2007**, 9.
[18] Motiwala H. F.; Vekariya R. H.; Aubé J. *Org. Lett.* **2015**, *17*, 5484.
[19] Katrizky A. R.; Zhang S.; Hussein A. H. M.; Fan Y.; Steel P. J. *J. Org. Chem.* **2001**, *66*, 5606.
[20] Owada M.; Sakiyama T.; Kitagawa T. *Pediatr. Res.* **1977**, *11*, 641.
[21] Lorincz M.; Herzenberg L. A.; Diwu Z.; Barranger J. A.; Kerr W. G. *Blood* **1997**, *89*, 3412.